Title	Corrective force analysis for scoliosis from implant rod deformation
Author(s)	Salmingo, Remel; Tadano, Shigeru; Fujisaki, Kazuhiro et al.
Citation	Clinical Biomechanics, 27(6), 545-550 https://doi.org/10.1016/j.clinbiomech.2012.01.004
Issue Date	2012-07
Doc URL	https://hdl.handle.net/2115/49633
Type	journal article
File Information	CB27_545-550.pdf

Corrective force analysis for scoliosis from implant rod deformation

Remel Salmingo, MEng [a], Shigeru Tadano, PhD [b,*], Kazuhiro Fujisaki, PhD [b],
Yuichiro Abe, MD, PhD [c], Manabu Ito, MD, PhD [c]

[a] *Division of Human Mechanical Systems and Design, Graduate School of Engineering, Hokkaido University, North 13 West 8 Kita-ku, Sapporo, Japan*

[b] *Division of Human Mechanical Systems and Design, Faculty of Engineering, Hokkaido University, North 13 West 8 Kita-ku, Sapporo, Japan*

[c] *Department of Orthopaedic Surgery, Graduate School of Medicine, Hokkaido University, North 15 West 7 Kita-ku, Sapporo, Japan*

[*] Corresponding Author

Shigeru Tadano,

e-mail: tadano@eng.hokudai.ac.jp

tel: +81117066405

fax: +81117066405

The total number of words of the main text excluding references: **3171**

The number of words of the abstract: **245**

The number of figures: **7**

The number of table: 1

ABSTRACT

Background: Scoliosis is a serious disease in which a human spine is abnormally deformed in three dimensions with vertebral rotation. Surgical treatment is attained when the scoliotic spine is corrected into its normal shape by implant rods and screws fixed into the vertebrae. The three-dimensional corrective forces acting at the screws deformed the implant rod during the surgical treatment of scoliosis. The objective of this study was to propose a method to analyze the three-dimensional forces acting at the rod using the changes of implant rod geometry before and after the surgical treatment.

Methods: An inverse method based on Finite Element Analysis is proposed. The geometries of implant rod before and after the surgical treatment were measured three-dimensionally. The implant rod before the surgical treatment was reconstructed using an elasto-plastic finite element model. The three-dimensional forces were applied iteratively to the rod through the screws such that the rod is deformed the same after the surgical treatment of scoliosis.

Findings: The maximum force acting at the screw of each patient ranged from 198 N to 439 N. The magnitude of forces were clinically acceptable. The maximum forces occurred at the lowest fixation level of vertebra of each patient.

Interpretation: The three-dimensional forces distribution that deformed the rod can be evaluated using the changes of implant geometry. Although the current clinical cases are still few, this study demonstrated the feasibility of measuring the forces that deformed the implant rod after the surgical treatment of scoliosis.

KEYWORDS

Biomechanics, scoliosis, rod deformation, finite element analysis

1. Introduction

Scoliosis is characterized as a three-dimensional (3D) deformity of the spine with axial rotation of the vertebrae. The degree of severity of the scoliotic deformity is evaluated using the value of Cobb angle. The Cobb angle is defined as the maximum angle between two lines drawn parallel to the endplates of scoliotic vertebrae at the frontal plane. The Cobb angle can be also expressed three-dimensionally (3D) using the method of (Kanayama et al., 1996). When the Cobb angle is greater than 50 degrees, surgical treatment using implant fixation is used.

Surgical treatment of severe scoliosis requires fixation of implantable devices such as rods, screws, hooks and wires accomplished using surgical techniques. Various rod rotation techniques have evolved and became more sophisticated in applying the forces required to correct the three-dimensional scoliotic deformity. These surgical techniques are rod rotation techniques or popularly known as Cotrel-Dubousset (CD) technique , Simultaneous Double Rod Rotation Technique (SDRRT) and other rod derotation techniques (Dubousset et al., 1988; Ito et al., 2010; Zielke, 1982; Cheng et al., 2008; Guidera et al., 1993, Mc Lain et al., 1993; Schlenk et al., 2003). The three-dimensional surgical correction of scoliosis is primarily dependent to the chosen surgical technique or procedure. The SDRRT procedure was used to correct the scoliosis deformity. In SDRRT, two pre-bent rods were inserted into the polyaxial screw heads. The polyaxial screw heads remained untightened until the rod rotation was completed (i.e. rod can rotate and translate freely inside the screw head during rod rotation maneuver). A rod rotating device was used to hold and rotate the rod. A torque was applied to the rod rotating device to rotate the rod (approx. 90°) at the same time to create corrective forces on rods through the screws to deform the spine into normal shape. Scoliosis correction was attained, however, the corrective

forces acting on screws were high enough that deformed the implant rod after the surgical treatment of scoliosis. Thus, investigation of the biomechanical changes (i.e. including forces that caused the deformation of implant rod in vivo) after the surgical procedure is important to understand the biomechanics of scoliosis correction. Understanding the biomechanics of scoliosis correction could help avoid clinical complications and obtain optimal surgical correction.

Several authors have investigated the biomechanics of scoliosis correction using patient-specific finite element models (Lafon et al., 2009; Wang et al., 2011). These studies were successful in analyzing the forces occurring at the implant rod-vertebra connection. However, the magnitude of forces obtained might not be so realistic because the analyses were focused only on the elastic deformation of rod. Elasto-plastic deformation analysis should have been considered. Furthermore, the rod geometry acquisition methods were limited because they did not measure the actual initial geometry of rod and the in vivo three-dimensional shape of the rod was just approximated from the postoperative radiographs and videos. Thus, it was not possible to obtain the real initial and final three-dimensional geometry of rod and consequently the forces using their methods.

The objective of this study was to propose a method to analyze the three-dimensional forces acting at each screw from the changes of implant geometry after scoliosis surgery using SDRRT. These forces could be the corrective forces developed at the screws transferred to rod due to the resistance of spine during the rod rotation maneuver. The method is based on FEA. The three-dimensional geometry of the implant rod was measured before and after surgery. The three-dimensional forces that deformed the rod could be obtained using just the geometry of rod before and after the surgical treatment of three scoliosis patients.

2. Methods

2.1 Force Analysis

Figure 1(left) shows the CT image of the spine after the surgical treatment in the posterior view. Figure 1(right) also shows the three-dimensional implant geometry of rod at the concave side before and after surgery. To standardize the use of the three-dimensional geometry of rod, the coordinate system proposed by the Scoliosis Research Society was used in this study (Yeung et al., 2003). The positive x-axis is directed anteriorly, the positive y-axis is directed toward the left lateral side and the positive z-axis is directed toward the superior direction. From a mechanical point of view, when a rod made from metal is deformed, forces occur in accordance to the deformation. This figure also shows that the implant rod at the concave side was deformed after surgery. It implies that there are forces acting at the implant rod after the surgical treatment of scoliosis.

Figure 2 is a schematic diagram showing implant rod deformation before and after surgery. The origin (0,0,0) was set at the inferior end of the rod. The three-dimensional force $\vec{F}_i$ acting at the screw (*i-th* from bottom) which displaced the position of screw before surgery $\vec{p}_i^0$ into after surgery $\vec{p}_i^*$ is required in the analysis. Initially, zero force is applied to the screw $\vec{p}_i^0$ on the rod geometry before surgery. The displacement $\vec{p}_i$ is calculated using FEA. To search for the forces acting at the deformed rod after surgery, the difference $\vec{e}_i$ which is defined as the distance between the screw location $\vec{p}_i^*$ on the rod geometry after surgery and displaced location $\vec{p}_i$ is used in the iteration process. The direction of the three-dimensional force $\vec{F}_i$ created from the x-z plane is defined as the angle θ_i. The

direction of force along *y-z* plane was neglected because CT acquisition could not accurately depict deformation along this plane.

Figure 3 shows the procedure to calculate the forces from implant rod deformation. Here, the three-dimensional rod geometries before and after surgery are already obtained. The rod diameter was 6mm and the rod length differs with each patient. The finite element model of the rod was made by ANSYS 11.0 software (ANSYS, Inc., Pennsylvania, USA) using a 10 node tetrahedral solid elements. The boundary condition was set considering the manner of rod fixation during the surgical treatment. The screws' coordinates were reoriented such that the most superior screw coincides with the z-axis (i.e. on top of the most inferior screw) because each patient has different implant rod orientation and fixation levels. The most inferior screw at the end of rod was fixed in all translations but free to rotate. The most superior screw was also fixed except that it was free to move along the superior direction only.

As the loading condition, Forces $\bar{F}_i$ were set with initial values. An elasto-plastic analysis was conducted since the implant rod was made from titanium alloy (JIS T 7401-3), a typical elasto-plastic material. The deformation behavior of the rod in uniaxial tensile loading is shown in Fig. 4. In the elastic region $(0 \le \varepsilon \le \varepsilon_Y)$, the stress-strain relation and E as the elastic modulus is expressed in Eq. (1)

$$\sigma = E\varepsilon \tag{1}$$

The stress-strain relationship in the plastic region $(\varepsilon_Y < \varepsilon)$ is expressed in Eq. (2). ε_Y is the yield strain indicating the start of plastic deformation.

$$\sigma = E\varepsilon_Y + H(\varepsilon - \varepsilon_Y) \tag{2}$$

Material properties of this rod are Young's Modulus (E), yield stress (σ_Y), yield strain (ε_Y) and hardening coefficient (H) equal to 105 GPa, 900 MPa, 8.57×10^{-3} and 2.41 GPa, respectively. In three-dimensional FE analysis, the von Mises stress was adopted to evaluate the stress distribution along the rod.

The displacements from elasto-plastic deformation $\vec{p}_i$ were analyzed using FEA. The difference $\vec{e}_i$ at each screw location was calculated from the screw location after surgery $\vec{p}_i^*$. The evaluating function which was defined as the sum of the squares of differences on each screw is expressed in Eq. (3).

$$\sum_{i=1}^{n} \left| \vec{e}_i \right|^2 < \alpha \tag{3}$$

If the evaluating function is greater than α (where $\alpha = 0.5$), the value of the applied forces $\vec{F}_i$ are replaced using Eq. (4) and iterated for the next step.

$$\vec{F}_i \leftarrow \vec{F}_i + \beta \, \vec{e}_i \tag{4}$$

The constant coefficient β in Eq. (4) is introduced in every iteration step so as to attain smooth and rapid convergence. The constant coefficient β is equal to 0.5 N·mm. The process was iterated until the value of Eq. (3) is less than α. The forces at this iteration step are considered to be optimal. These forces could be the result of corrective forces transferred to the spine since the rod is directly attached to it through the screws. Furthermore, the stress or strain distributions in the deformed implant rod caused by the forces $\vec{F}_i$ were obtained in this study.

2.2 Clinical Geometry Measurements

The initial geometry of implant rod was measured from the actual rod used before surgery. The implant rod geometry after surgery was obtained a week after the surgical operation using Aquilion 64 CT scanner (Toshiba Medical Systems Corporation, Tochigi, Japan). The slice thickness was 0.5mm. The images were

imported into CAD software Solidworks 2010 (Dassault Systemes, Massachusetts, USA) to measure the 3D geometry and deformation. The procedure was approved by the ethics committee of Graduate School of Medicine. A proper informed consent was obtained for all patients. All patients were classified as severe Adolescent Idiopathic Scoliosis (AIS) that is with high Cobb angle which requires surgical treatment. The USS II 6 mm diameter rods and polyaxial pedicle screws (Synthes GmbH, Oberdorf, Switzerland) were implanted using the SDRRT surgical technique. The clinical data of the patients used in this study is listed in Table 1.

In SDRRT, two implant rods were used. However, in all patients, the rod geometry images show that the rod at the convex side was not deformed (i.e. minimum and rod deformation cannot be detected by CT imaging) after the surgical treatment of scoliosis. This implies that the corrective force acting on the rod at the convex side was negligible. On the other hand, the rod at the concave side was significantly deformed. The three-dimensional changes of rod geometry at the concave side of the three patients were used to analyze the forces acting at the rod after the surgical treatment of scoliosis.

3. Results

3.1 Forces Analysis

The iteration process was stopped when the objective function was less than α. The applied forces at this iteration step is referred to as the optimal forces $\bar{F}_i$. Figure 5(top) shows the magnitude of three-dimensional forces acting at the vertebrae of Patient 1. The direction of the three dimensional forces at each level of vertebra along the x-z plane is defined by angle θ_i. The direction of forces along the y-z plane was neglected since the rod was not deformed along that

plane. Figure 5(bottom) shows the magnitude of forces that deformed the rod for Patient 2 and Patient 3. The maximum forces obtained were 248 N, 198 N and 439 N for Patient 1, Patient 2 and Patient 3 respectively.

3.2 Stress Distribution

To identify the possible location of rod breakage, the von Mises stress distributions were also obtained using FEA. Figure 6 shows the von Mises stress distributions when the implant rod was deformed after the surgical treatment of scoliosis. The maximum von Mises stresses were 726 MPa, 241 MPa, 905 MPa located at T10 for Patient 1, T11 for Patient 2, T11 for Patient 3 respectively.

4. Discussion

The forces acting at each screw were calculated using just the changes of implant rod geometry before and after surgery using SDRRT. The current maximum values obtained in this study were at the lumbar region 248 N, 198 N and 439 N for Patient 1, Patient 2 and Patient 3 respectively. These forces occurred at each screw when the scoliotic spine resists the rotation of rod. As a result, the forces deformed the rod after the surgical treatment of scoliosis. These forces could be the result of corrective forces transferred to the rod and vertebrae of spine since it is attached into the screws.

The present method could be used also to analyze the post-operative corrective forces from the changes of implant rod geometry after many months or years. These could be done by taking CT images of implant rod. Post-operative daily living activities such as standing, bending, walking and etc. may change the rod shape as well as the corrective forces acting on it. These activities may cause corrective forces to increase or decrease which may affect the stability of the fixation. Furthermore, these activities could also develop high corrective forces

which might be unsafe to the patient. Thus, the present method will be applied to investigate the magnitude of post-operative corrective forces from the changes of implant rod geometry during future patient follow ups.

The objective of scoliosis correction is to deform and fix the scoliotic spine into its normal shape without damaging deformations and neurological complications. This could be attained by applying suitable corrective forces to the spine through implant rods and screws. The corrective forces required to correct the deformity must be sufficient in order to achieve the required correction. Lou et al. attached strain gages to the rod rotating device. They monitored the corrective force applied by surgeon at the rotating device during the CD derotation maneuver. The measured corrective force ranged from 22-57 N (Lou et al., 2002). Although patients were limited, an increasing trend was found between the applied force and degree of correction. However, the corrective forces acting at each screw were difficult to measure since the rotating device is attached only to the implant rod. The magnitude of forces occurring at each screw is also important because overloading due to the rod rotation maneuver might occur (Little and Adam, 2010).

Another important issue during the rod rotation maneuver is the loss of feeling of the surgeon to feel the resistance of each corrected level (i.e. located at each screw). This is because the rod rotating device is attached to the rod at a single location only. The corrective forces occurring at each screw might be excessive (Lou et al., 2002). 15 cases of pedicle fractures were reported during the rod rotation maneuver due to excessive corrective forces (Di Silvestre et al., 2007). Although it is difficult, however, it will be more meaningful for future studies if we can directly establish the relation of the required torque to rotate the rod and the forces acting on each screw or vice versa. From this, the surgeons can

decide intraoperatively whether the applied torque during the rotation maneuver is safe or not.

Some cases of broken implant rods were reported during CD instrumentation (Guidera et al., 1993). The breakage risk was investigated using von Mises stress. The von Mises stress distribution along the entire length of the deformed rod was obtained. The possible locations of rod breakage can be located. This also demonstrates the usefulness of the current method to locate possible locations of implant rod fracture by checking the stresses distribution after the surgical treatment of scoliosis.

Accurate measurement of implant rod geometry before the surgical treatment is important to attain more accurate results. Currently, the surgeons manually traced the contoured rods using the actual implant rod used before surgery. The traced geometry was scanned and reconstructed as an image file. The CT imaging can be used also to measure the rod geometry before surgery. Although this has not been done yet, we have to consider its viability in the clinical setting. Furthermore, a precise 3D geometry measurement method can be developed using laser displacement sensors. Laser displacement sensor is useful clinically because it can measure the shape of the rod without contact.

The scoliosis cases presented here shows that the screws were not inserted at all vertebral levels. The forces might change if more or lesser screws were used. Thus, there can be various screw placement configurations applicable for a certain scoliosis case. Some authors investigated the different screw placement configurations in anterior spine instrumentation using a biomechanical model (Desroches et al., 2007). They were successful in finding the optimal screw placement configurations before surgery as confirmed by their post operative results. Likewise, some screw placement configurations were not recommended

because their calculated corrective forces exceeded the published pullout forces. Their study introduces the possibility to perform preoperative planning using the anterior approach. Further study considering not only the deformation of rod but also the effect of various screw placement configuration to the corrective forces in SDRRT surgical technique shall be further investigated (e.g. optimal number of screws and placement of screws).

The current method presented here calculated the corrective forces acting at the implant rod after the surgical treatment of scoliosis. Lou et al., 2002 strengthened that too much high corrective forces can cause implant breakage or bone fracture which may lead to pullout of screws from the vertebra. Thus, the magnitude of corrective forces is critical during surgery. Liljenqvist et al., 2001 performed biomechanical pullout tests of pedicle screws using nine human cadaveric thoracic spines. The measured pullout strengths of the pedicle screws ranged from 532 N to 808 N (Liljenqvist et al., 2001). Although this value seems to be unsafe because it is close to the maximum calculated value of our study (i.e. 439 N), implant differences as well as specimen (osteoporotic vs. normal, age, sex) need to be considered for better comparison. The closest pullout experiment that can be compared to our results was conducted by Seller et al., 2007. They performed pullout test using calf vertebrae and the same implant screw used in our study (i.e. USS II posterior screw). The average pullout force was 2413 N that was approximately 5.5 times higher than the maximum calculated force of our study (2413 N / 439 N ≈ 5.5). This suggests that the forces acting on the screws of the current scoliosis cases are still safely below the pullout force threshold. Although differences in bone quality and implant configurations such as implant insertion depth might affect the comparison, actual pullout

experiments shall be conducted to validate these findings. Nevertheless, problems involving screw pullout did not occur as confirmed by the surgeons.

In the current treatment, two rods were used for each case. The geometry of rod attached in the concave and convex side of Patient 1 is shown in Figure 7. The rod geometry of all patients at the convex side was not deformed after the surgical treatment. Although the current numbers of cases were few, further investigation must be made in order to elucidate the mechanism of these findings. Conversely, the rod at the concave side indicates that it has a significant mechanical role during the SDRRT.

In surgically treated scoliotic patients, the implant rod and screw are fixed into the spine for a long period of time. The bone of the spine is continuously remodeling or adapting its structure during the fixation period. At this time, the forces acting on the rod might change due to adaptation of spine. The changes of rod geometry will be further investigated using CT imaging during future follow-ups.

5. Conclusion

In this study, the distributions of forces that deformed the implant rod were analyzed using just the rod geometry before and after the surgical treatment. These forces could be associated with the corrective forces acting at the vertebrae of the spine since the rod is directly attached to it through the screws. The work presented here helps to understand the magnitude of corrective forces acting at the vertebrae of spine during scoliosis correction surgery. Future studies involving larger number of patients will elucidate the relationship between the corrective forces acting at the rod and scoliosis correction mechanism.

References

Cheng, J., Lebow, R., Schmidt, M., Spooner, J., 2008. Rod derotation techniques for thoracolumbar spinal deformity. Neurosurgery. 63, 149-156.

Cotrel, Y., Dubousset, J., Guillaumat, M., 1988. New universal instrumentation in spinal surgery. Clin. Orthop. 227, 10-23.

Desroches, G., Aubin, C., Sucato, D., Rivard, C., 2007. Simulation of an anterior spine instrumentation in adolescent idiopathic scoliosis using a flexible multi-body model. Med. Bio. Eng. Comput. 45, 759-768.

Di Silvestre, M., Parisini, P., Lolli, F., Bakaloudis, G., 2007. Complications of thoracic pedicle screws in scoliosis treatment. Spine. 32, 1655-1661.

Guidera, K., Hooten, J., Weatherly, W., Highhouse, M., Castellvi, A., Ogden, J., Pug, L., Cook, S., 1993. Cotrel-Dubousset instrumentation: results in 52 patients. Spine. 18, 427-431.

Ito, M., Abumi, K., Kotani, Y., Takahata, M., Sudo, H., Hojo, Y., Minami, A., 2010. Simultaneous double rod rotation technique in posterior instrumentation surgery for correction of adolescent idiopathic scoliosis. J. Neurosurg. Spine. 12, 293–300.

Kanayama, M., Tadano, S., Kaneda, K., Ukai, T., Abumi, K., 1996. A mathematical expression of three-dimensional configuration of the scoliotic spine. J. Biomech. Eng. 118, 247-52.

Lafon, Y., Lafage, V., Dubousset, J., Skalli, W., 2009. Intraoperative three-dimensional correction during rod rotation technique. Spine. 34, 512-519.

Liljenqvist, U., Hackenberg, L., Link, T., Halm, H., 2001. Pullout strength of pedicle screws versus pedicle and laminar hooks in the thoracic spine. Acta Orthopaedica Belgica. 67, 157-163.

Little, J., Adam, C., 2010. Development of a computer simulation tool for application in adolescent spinal deformity surgery. Lecture Notes in Computer Science. 5958, 90-97.

Lou, E., Hill, D., Raso, J., Moreau, M., Mahood, J., 2002. Instrumented rod rotator system for spinal surgery. Med. Biol. Eng. Comput. 40, 376-379.

McLain, R.F., Sparling, E., Benson, D.R., 1993. Early failure of short-segment pedicle instrumentation for thoracolumbar fractures. A preliminary report. J. Bone Joint Surg. Am. 75, 162-167.

Schlenk, R.P., Kowalski, R.J., Benzel, E.C., 2003. Biomechanics of spinal deformity. Neurosurg. Focus. 14, 1-6.

Seller, K., Wahl, D., Wild, A., Krasupe, R., Schneider, E., Linke, B., 2007. Pullout strength of anterior spinal instrumentation: a product comparison of seven screws in calf vertebral bodies. Eur. Spine J. 16, 1047-1054.

Wang, X., Aubin, C., Crandall, D., Labelle, H., 2011. Biomechanical modeling and analysis of a direct incremental segmental translation system for the instrumentation of scoliotic deformities. Clin. Biomech. 26, 548-555.

Yeung, A., Ottaviano, D., Lee, D., Haher T., 2003. Spine testing modalities, in: DeWald, R., Arlet, V., Carl, A., O'Brien, M., (Eds.), Spinal deformities the comprehensive text, Thieme Medical Publishers Inc., New York, pp. 176-186.

Zielke, K., 1982. Ventral derotation spondylodesis. Results of treatment of cases of idiopathic lumbar scoliosis. Z. Orthop. Ihre. Grenzgeb. 120, 320–329.

List of Tables

List of Figures

Figure 1 Image showing 3D implant rod deformation before and after the surgical treatment

CT image of the spine and rods fixed by the screws

3D geometry of deformed rod and force at fixation point shown in frontal and sagittal view
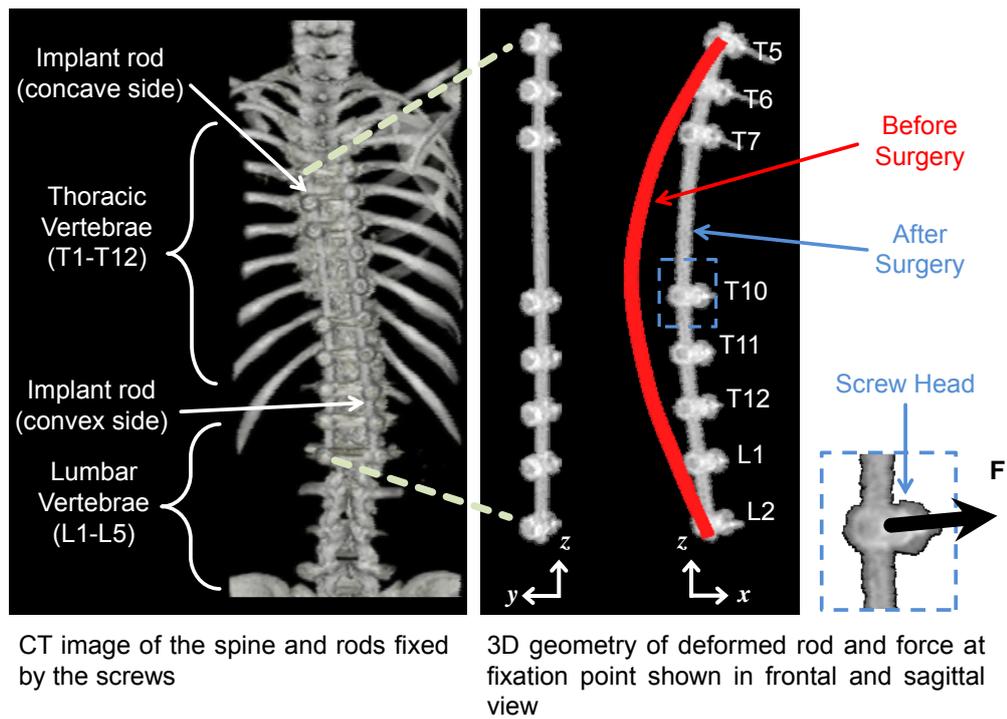
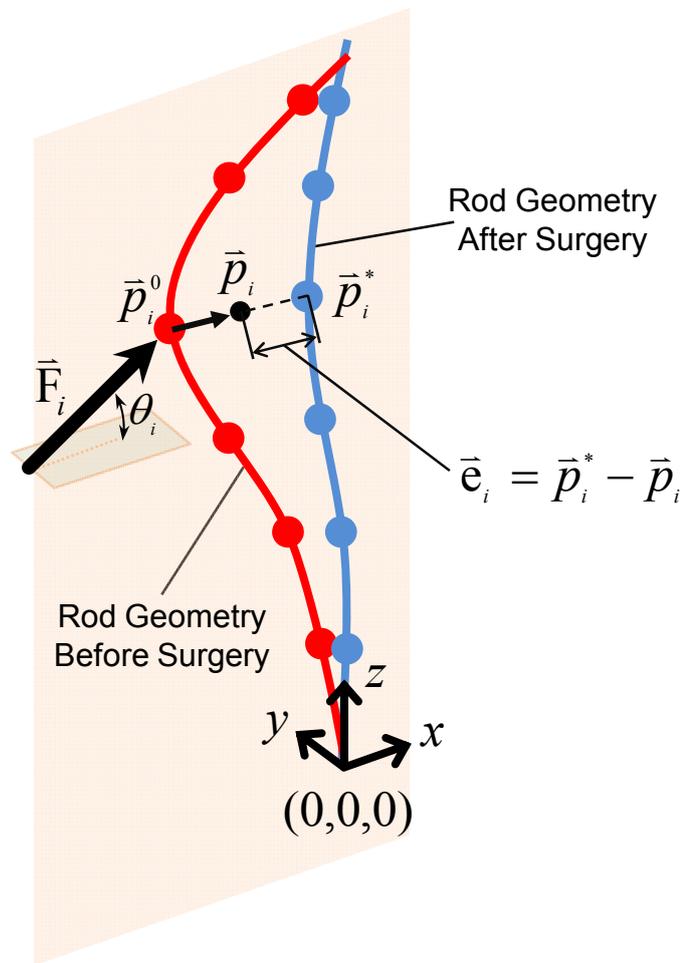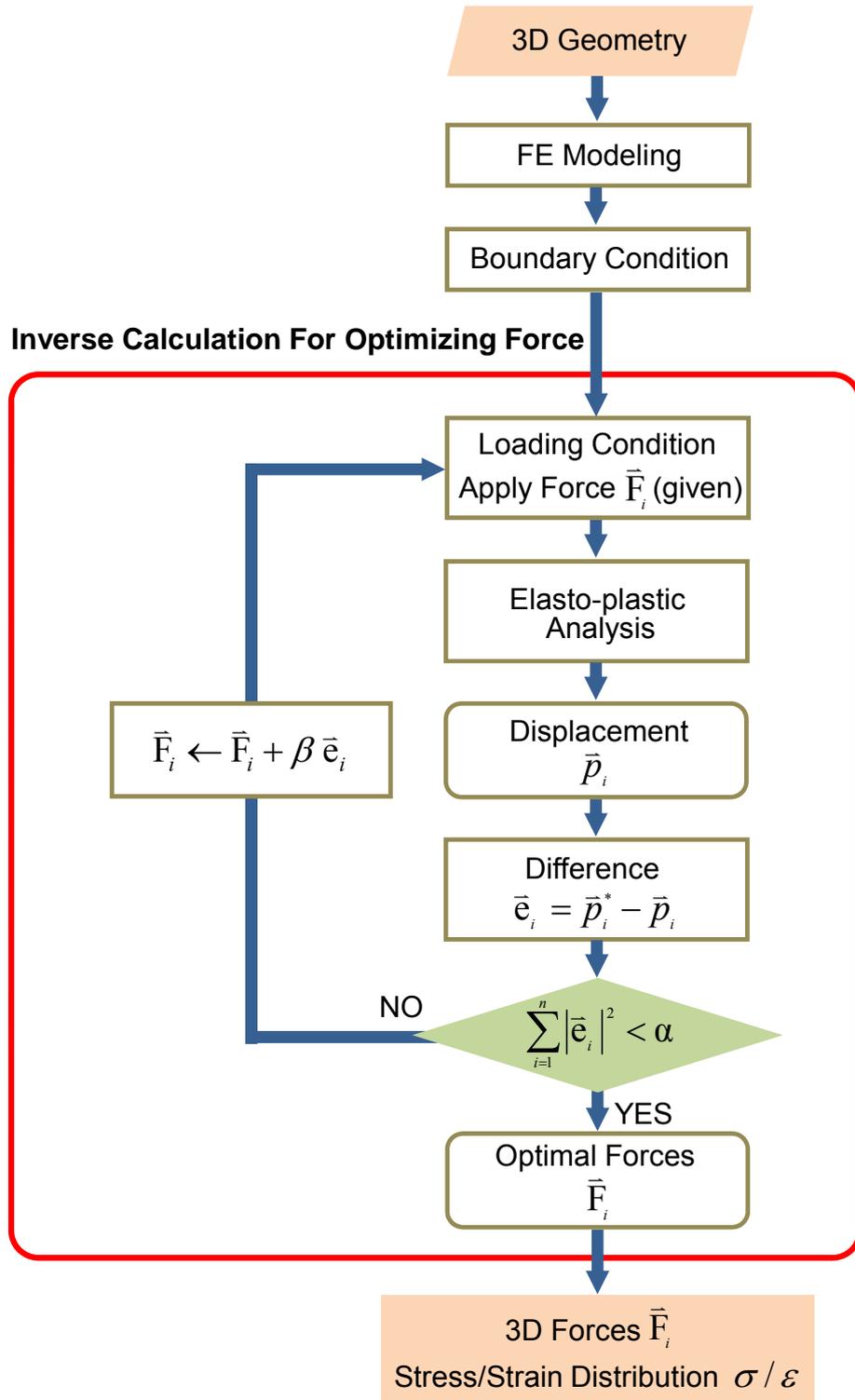**Figure 2** Schematic diagram of 3D rod geometry before and after surgery

Figure 3 Procedure for 3D force analysis
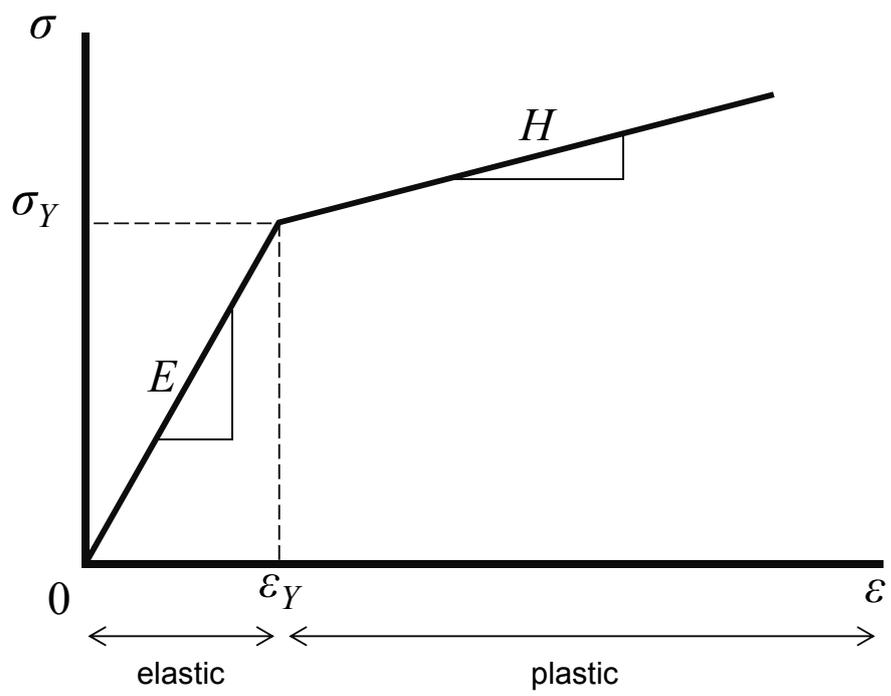
Figure 4 Bilinear elasto-plastic material model

Figure 5 Magnitude of 3D forces at each screw calculated from implant rod deformation
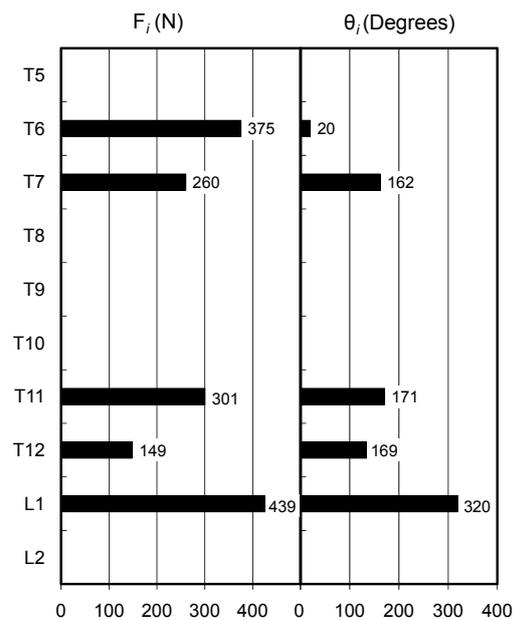

Tadano Figure 5
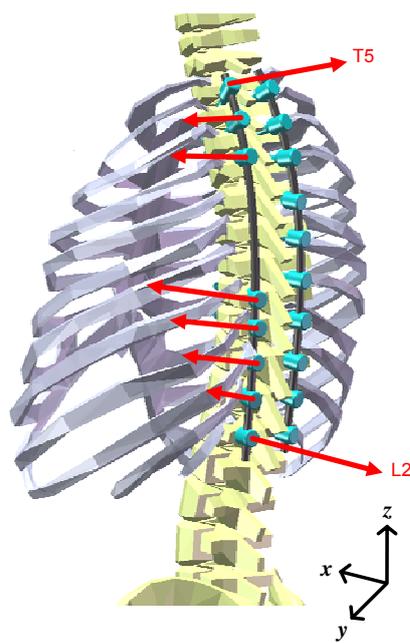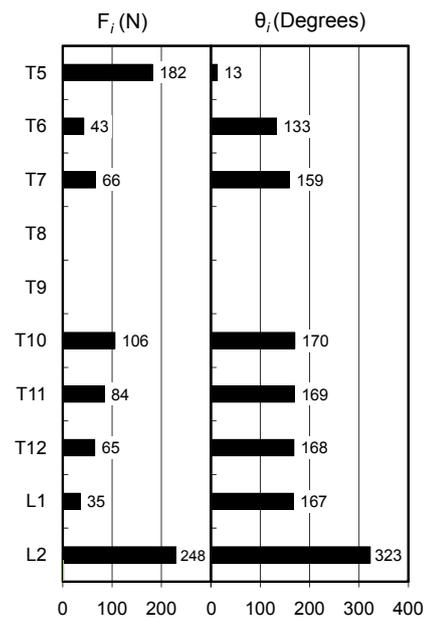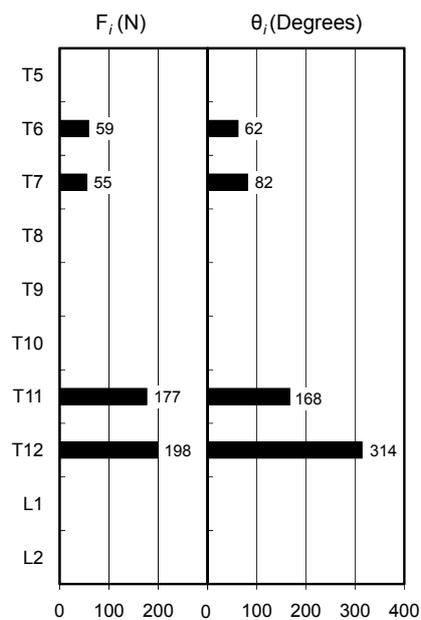
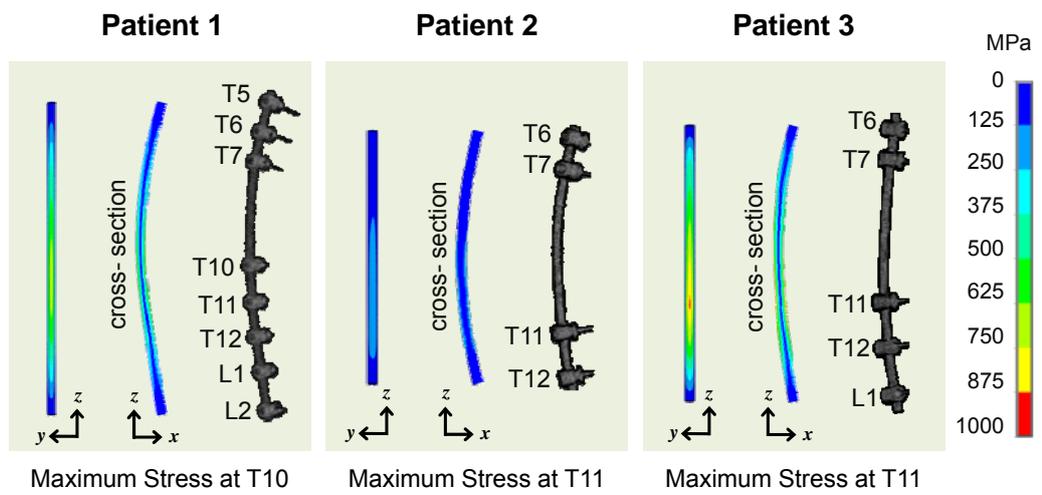**Figure 6** von Mises stress distribution of deformed rod after the surgical treatment

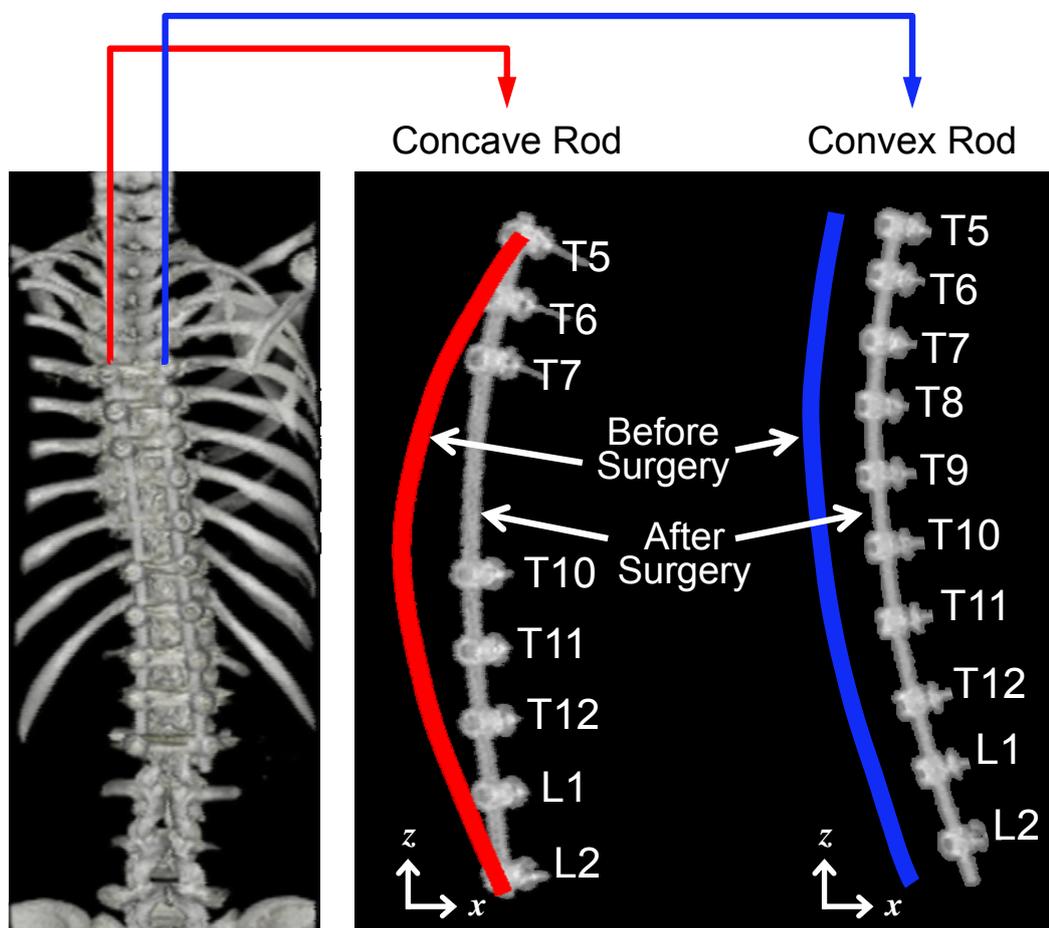**Figure 7** Rod geometries in the concave and convex side before and after the surgical treatment of Patient 1

Table 1 Clinical data of the three scoliotic patients

Scoliosis	Gender	Age	Cobb angle before surgery	Cobb angle after surgery	Screw locations at vertebra	Length of Rod (mm)
Patient 1	Female	16	57°	13°	T5, T6, T7, T10, T11, T12, L1, L2	226 (T5 to L2)
Patient 2	Female	15	59°	28°	T6, T7, T11, T12	159 (T6 to T12)
Patient 3	Female	14	68°	18°	T6, T7, T11, T12, L1	177 (T6 to L1)